NACA

RESEARCH MEMORANDUM

INVESTIGATION OF A TRANSLATING-CONE INLET AT

MACH NUMBERS FROM 1.5 TO 2.0

By L. Abbott Leissler and William H. Sterbentz

Lewis Flight Propulsion Laboratory
Cleveland, Ohio

NATIONAL ADVISORY COMMITTEE
FOR AERONAUTICS
WASHINGTON
May 11, 1954

NATIONAL ADVISORY COMMITTEE FOR AERONAUTICS

RESEARCH MEMORANDUM

INVESTIGATION OF A TRANSLATING-CONE INLET AT

MACH NUMBERS FROM 1.5 TO 2.0

By L. Abbott Leissler and William H. Sterbentz

SUMMARY

An investigation was conducted in the Lewis 8- by 6-foot supersonic wind tunnel to evaluate the performance of a translating-cone inlet operated over the Mach number range from 1.5 to 2.0 and angles of attack to 9°. The effects of spike projection and internal flow area variation on pressure recovery, external drag, and corrected air-flow variation were determined.

Either external flow reexpansion over the translating cone shoulder or internal flow contraction decreased the diffuser pressure recovery and, in general, increased the external drag. In addition, internal flow contraction seriously limited the variation in corrected air flow that could be obtained at critical flow conditions. Nevertheless, a translating-cone diffuser showed performance gains over fixed-geometry inlets where a variation in corrected air flow with free-stream Mach number was desired.

INTRODUCTION

Most modern aircraft jet engines are required to deliver propulsive thrust efficiently over a range of flight conditions. One condition necessary to the accomplishment of this task is a variable mass flow. If the over-all efficiency of the complete engine and inlet combination is to remain high, the inlet must deliver the engine air-flow requirement at peak or near-peak performance. Several schemes have been suggested for efficiently varying the mass flow to a jet engine, and these are discussed in references 1 to 6. One scheme employs a translating compression surface which for conical spike diffusers would be a translating cone.

Some examples of translating-cone inlets are discussed and experimentally evaluated in references 5 and 6. A factor not evaluated to date is the selection of the proper conical spike projection and internal flow area variation for most effective performance over a given mass-flow

schedule. To obtain some information on this problem, nine combinations
of diffuser cowl and spike projections derived from three diffuser designs
were studied.

The experimental investigation reported herein evaluates the exter-
nal drag, pressure recovery, and corrected air-flow variation for the
nine cowl and spike projection combinations at zero angle of attack and
free-stream Mach numbers from 1.5 to 2.0. The variation of pressure
recovery with mass-flow ratio and corrected air flow was also obtained
at angles of attack to 9°. From these data, some performance limitations
of spike projection and internal flow area variation are noted. Also,
a comparison of the performance of translating-spike diffusers with that
of fixed-spike diffusers is presented.

SYMBOLS

The following symbols are used in this report:

A   area

A_4 maximum flow area (0.289 sq ft)

$A_{4,1}$ diffuser discharge area, sting out (0.338 sq ft)

C_D drag coefficient, $D/q_0 A_{max}$

D   external drag including additive drag

L   length of model shell (55.8 in.)

M   Mach number

m/m_0 mass-flow ratio (actual mass flow$/\rho_0 V_0 A_1$)

P   total pressure

p   static pressure

q   dynamic pressure, $\dfrac{\gamma p M^2}{2}$

T   total temperature

W   air flow

W_{ac} corrected air flow per unit area, $W \sqrt{\theta}/A_{4,1}\delta$

α angle of attack

γ ratio of specific heats for air (1.4)

3206

CK-1 back

δ ratio of P_3 to NACA standard sea-level absolute pressure

θ ratio of T_3 to NACA standard sea-level absolute temperature

ρ mass density of air

Subscript:

max maximum external diameter

Stations:

x longitudinal location

0 free stream

1 leading edge of cowl lip

3 plane of survey

4 diffuser discharge at constant diameter section

4,1 diffuser discharge at constant diameter section, sting out

APPARATUS AND PROCEDURE

The model was sting-mounted in the Lewis 8- by 6-foot supersonic tunnel. Over-all dimensions and general internal contours of the model are given in figure 1. A movable plug at the exit was used to vary the mass flow through the model.

Nine combinations of diffuser cowl and spike projections derived from three diffuser designs were investigated. Each of the three diffusers was designed to have the same basic internal flow area variation (fig. 2) and to intercept the oblique shock generated by the cone (25° half-angle) at the cowl lip at one of the free-stream Mach numbers 1.5, 1.8, or 2.0. By translating the conical spike of each of these three basic diffusers by means of fixed spacers, the total of nine combinations was obtained. A schematic sketch of each combination and the resulting diffuser area variation are given in figure 3 and table I.

Each of the nine diffuser configurations is designated by a number such that the first two figures denote the Mach number for which the inlet and subsonic diffuser combination are nearly optimum and the last two numbers denote the Mach number at which the oblique shock generated by the cone would intersect the cowl lip. Thus, the 2020 inlet has the cowl and spike combination designed for Mach number 2.0 with spike set

at the position for oblique shock-cowl lip intersection at 2.0. The 2015 inlet has the same cowl and cone as for the 2020 inlet, but with the cone translated and set for oblique shock-cowl lip intersection at Mach number 1.5.

The instrumentation of the model included a three-component strain gage balance located within the model center body to determine model drag forces, a dynamic pressure pickup and recorder to determine the onset of diffuser buzz, a remote-reading pendulum-type attitude indicator to determine angle of attack, and a static pressure survey for determining mass flow (sonic-flow area method) and diffuser total-pressure recovery. The wind tunnel schlieren system was used to obtain photographs of the shock pattern generated by the inlets.

Experimental data were obtained for each of the nine configurations over a range of mass-flow ratios at Mach numbers 1.5, 1.8, and 2.0 and angles of attack of 0°, 3°, 6°, and 9°. Drag coefficients determined from the investigation are based on a maximum model frontal area of 0.360 square feet. The free-stream Reynolds number based on the maximum model diameter was about 3.4×10^6.

RESULTS AND DISCUSSION

The pressure recovery and drag of the nine inlet combinations as a function of mass-flow ratio at zero angle of attack is presented in figures 4 to 6. The variation of pressure recovery with angle of attack is shown in figures 7 to 9. Schlieren photographs of the shock wave patterns generated by the inlet for some flow conditions are shown in figures 10 to 12.

In the design of translating-spike inlets, some compromise in performance is necessary in the variable speed range. If the inlet is designed with a low-drag cowl, then spike translation from the design point may cause either internal contraction or flow reexpansion due to projections of the spike shoulder ahead of the cowl lip. For inlets investigated herein, it was decided to accept these compromises rather than to include a higher cowl drag at the design point.

Flow Reexpansion

Effects of flow reexpansion over the cone shoulder as the cone is projected ahead of the inlet are illustrated by the data obtained for the 2020 and 1520 inlets (see figs. 4(a) and 6(a)). At a free-stream Mach number of 2.0 and zero angle of attack, the 2020 inlet (without reexpansion, fig. 10(a)) had a critical flow pressure recovery of 84 percent and an external drag coefficient of 0.11. The 1520 inlet, which has the

3206

cone shoulder projected ahead of the cowl lip (fig. 10(b)), has a critical flow pressure recovery of 81.5 percent and an external drag coefficient of 0.11. Thus, pressure recovery is adversely affected by flow reexpansion occurring over the cone shoulder projected ahead of the cowl lip.

Internal Contraction

The experimental results for the 20-series inlets (one cowl, three spike positions - figs. 4(a), (b), and (c)) illustrate the losses encountered as a result of internal contraction. At a free-stream Mach number of 1.5, the 2020 inlet (without internal contraction, fig. 11(a)) has a critical flow pressure recovery of 91 percent and a drag coefficient of 0.14. As the conical spike was progressively retracted to the 2018 (fig. 11(b)) and the 2015 positions, with resulting progressively greater internal contraction, the critical flow pressure recovery was reduced to 90.5 percent and 88 percent, respectively. The drag coefficient increased to 0.15 and 0.16, respectively.

Oblique Shock Within Lip

Also of interest is the flow condition for which the oblique shock from the cone falls within the cowl lip. At a free-stream Mach number of 2.0, the 1820 inlet (oblique shock at cowl lip, fig. 12(a)) had a critical flow pressure recovery of 82.5 percent compared with 79.0 percent for the 1818 inlet (fig. 12(b)), which has the spike retracted so that the oblique shock falls within the inlet lip. No change in inlet drag was obtained. The slight variation in critical mass-flow ratio is believed to be within the accuracy of the data.

The experimental data thus far discussed were obtained with spacers designed to give smooth centerbody contours. However, actual translating cone diffusers will generally incorporate a short cylindrical section as an aid to mechanical translation. Insertion of spacers having a cylindrical section on the 1520 and 1518 inlets (fig. 3(a)) to simulate the centerbody contour to be expected for an actual translating-cone diffuser had no adverse effects on diffuser performance (figs. 6(a) and 6(b)).

General Performance Comparison

Engines and inlets may be matched on a basis of a corrected air-flow parameter $\frac{W\sqrt{\theta}}{\delta}$ (ref. 7). Optimum matching of engine and inlet is obtained when the inlet supplies the engine corrected air-flow requirement at highest pressure recovery and lowest drag. This condition is generally

satisfied at critical flow operation of the inlet. For a better evalu-
ation of the characteristics of these translating-cone inlet designs,
the critical flow data of figures 4 to 9 are plotted as a function of
the corrected air-flow parameter in figures 13 and 14. The solid lines
indicate the variation of pressure recovery or external drag coefficient
at a constant free-stream Mach number as the cone is either retracted or
projected. The dashed curves indicate the variation of these quantities
with free-stream Mach number for a fixed cone setting, that is, a fixed-
geometry inlet.

Constant Mach number operation . - With the 15-series inlet (having
no internal contraction), it was possible to obtain approximately a 15
percent variation in corrected air flow at a free-stream Mach number of
1.5 while maintaining critical flow conditions (see fig. 13(c)). When
the conical spike was translated for the 15-series inlet, the cone
shoulder was always ahead of the cowl lip. Thus, although the flow
reexpansion generated by the cone shoulder penalized the general level
of pressure recovery, no difficulty was experienced in obtaining a
reasonable degree of variation in the corrected air flow. However, for
the 20-series inlet (fig. 13(a)) for which the cone shoulder was always
contained within the cowl lip, the internal flow contraction limited
the variation in corrected air flow obtainable at critical flow conditions
to only 2.6 percent at a free-stream Mach number of 1.5. Furthermore,
an additional penalty associated with this inlet compared with the 15-
series inlet was a considerably higher external drag.

The wider range of corrected air flow obtained at a free-stream
Mach number of 2.0 for the 20-series inlet arises principally from
the greater variation in diffuser pressure recovery and flow spill-
age behind a bow shock obtained by spike translation. Corrected air
flow variation obtained in this manner is, of course, undesirable because
of the large losses in pressure recovery and increases in drag which are
incurred. These data therefore demonstrate that internal flow contraction
defeats the purpose of a translating-spike inlet.

Angle of attack performance. - Shown in figure 14 is the variation
of pressure recovery as a function of the corrected air flow parameter
for critical flow conditions at an angle of attack of 9°. A comparison
of these maps with those of figure 13 shows the change in corrected
air-flow parameter that occurs with a change in angle of attack. In
most instances, only a small adjustment in translation of the conical
spike would be required to correct for the change in corrected air flow
which arises in changing the angle of attack from 0° to 9°. At 9° angle
of attack there is, as might be expected, a generally lower level of
pressure recovery.

Variable Mach number operation. - A comparison of the performance of
the translating 15-series inlet with that of the 1520 and 2020 fixed-
geometry inlets is shown in figure 15. The corrected air-flow schedule
with free-stream Mach number selected for matching corresponds to the

3206

variation of corrected air flow for the translating 15-series inlet when the oblique shock generated by the cone intersects the cowl lip. This air-flow schedule follows the trend usually expected for a turbojet engine operating over a range of Mach numbers at a constant corrected rotational speed.

At a free-stream Mach number of 1.5, the pressure recovery of the 15-series translating-cone inlet was 4.8 percent lower than that for the 2020 inlet. However, this lower pressure recovery for the translating-spike inlet was accompanied by a 17 percent lower external drag coefficient. As the free-stream Mach number is increased, the fixed-geometry inlet delivers too much air and must operate subcritically. Thus, at a free-stream Mach number of 2.0, the translating-cone inlet has a 41 percent lower external drag while maintaining a diffuser pressure recovery within 2 percent of that for the 2020 inlet. Also, the 1520 inlet has approached its subcritical diffuser stability limit, presenting additional difficulties of operation with this particular diffuser. These comparisons, of course, could be altered if an engine schedule was used that differed from that of this example.

SUMMARY OF RESULTS

An investigation of a translating-conical-spike diffuser over a free-stream Mach number range from 1.5 to 2.0 gave the following results:

1. External flow reexpansion over the diffuser cone shoulder, internal flow contraction, or location of the oblique shock within the cowl lip caused a decrease in diffuser pressure recovery and, in some instances, increases in external drag. In addition, internal flow contraction limited the critical flow corrected air-flow variation obtained by spike translation to only 2.6 percent at a free-stream Mach number of 1.5.

2. A translating-cone diffuser showed performance gains over fixed-geometry inlets where a variation in corrected air flow with free-stream Mach number was desired. At a free-stream Mach number of 2.0, while maintaining pressure recovery to within 2 percent of that attained with a fixed-geometry inlet, the translating-cone diffuser had approximately 41 percent lower external drag.

Lewis Flight Propulsion Laboratory
  National Advisory Committee for Aeronautics
    Cleveland, Ohio, March 11, 1954

REFERENCES

1. Allen, J. L., and Beke, Andrew: Force and Pressure Recovery Characteristics at Supersonic Speeds of a Conical Spike Inlet with Bypasses Discharging in an Axial Direction. NACA RM E52K14, 1953.

2. Hayes, Clyde: Preliminary Investigation of a Variable Mass-Flow Supersonic Nose Inlet. NACA RM L9J11, 1949.

3. Schueller, Carl F., and Esenwein, Fred T.: Analytical and Experimental Investigation of Inlet-Engine Matching for Turbojet-Powered Aircraft at Mach Numbers Up to 2.0. NACA RM E51K20, 1952.

4. Bernstein, Harry, and Haefeli, Rudolph C.: Performance of Isentropic-Forebody Nose Inlets at Mach Number of 5.6. NACA RM E54B24, 1954

5. Hinners, Arthur H., Jr., and Lee, John B.: Preliminary Investigation of the Total-Pressure-Recovery Characteristics of a 15° Semiangle Movable-Cone Variable-Geometry Ram-Jet Inlet at Free-Jet Mach Numbers of 1.62, 2.00, 2.53, and 3.05. NACA RM L52K10, 1953.

6. Gorton, Gerald C.: Investigation of Translating-Spike Supersonic Inlet as Means of Mass-Flow Control at Mach Numbers of 1.5, 1.8, and 2.0. NACA RM E53G10, 1953.

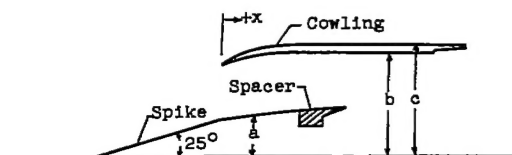7. Wyatt, DeMarquis D.: An Analysis of Turbojet-Engine-Inlet Matching. NACA TN 3012, 1953.

3206

3206

CK-2

TABLE I. - COORDINATES OF DIFFUSER COWLS, CONES, AND SPACERS

[Dimensions are in inches.]

20-series inlets

Cowling

x	b	c
0	2.66	2.66
.25	2.69	2.74
.50	2.73	2.79
1.00	2.80	2.89
2.00	2.93	3.04
3.00	3.04	3.16
4.00	3.13	3.25
5.00	3.20	3.32
6.00	3.25	3.38
7.00	3.30	3.42
8.00	3.33	3.45
8.67	3.35	3.47

Spike

a	x		
	Inlet 2020	Inlet 2018	Inlet 2015
0[1]	-2.86	-2.58	-1.93
1.32[1]	0.00	.28	.93
1.39	.20	.48	1.13
1.45	1.40	.68	1.33
1.51	.60	.88	1.53
1.61	1.00	1.28	1.93
1.84	2.00	2.28	2.93
2.01	3.00	3.28	3.93
2.14	4.00	4.28	4.93
2.24	4.94	5.22	5.87

Spacers

Inlet 2020		Inlet 2018		Inlet 2015	
a	x	a	x	a	x
2.24	4.94	2.24	5.22	2.24	5.87
2.31	5.94	2.31	6.22	2.31	6.87
2.37	6.94	2.38	7.22	2.40	7.67
2.40	7.67	2.40	7.67	----	----

18-series inlets

Cowling

x	b	c
0	2.55	2.55
.25	2.58	2.60
.50	2.61	2.64
1.00	2.67	2.74
2.00	2.80	2.92
3.00	2.92	3.04
4.60	3.12	3.24
5.60	3.22	3.34
7.60	3.29	3.41
8.67	3.35	3.47

Spike

a	x		
	Inlet 1820	Inlet 1818	Inlet 1815
0[1]	-2.74	-2.41	-1.79
1.12[1]	-.33	.00	.618
1.16	-.23	.1	.72
1.21	-.08	.25	.87
1.26	.07	.4	1.02
1.42	.77	1.1	1.72
1.64	1.77	2.1	2.72
1.84	2.77	3.1	3.72
2.03	3.77	4.1	4.72
2.21	4.85	5.18	5.80

Spacers

Inlet 1820		Inlet 1818		Inlet 1815	
a	x	a	x	a	x
2.21	4.85	2.21	5.18	2.21	5.80
2.31	5.65	2.31	5.98	2.31	6.60
2.37	6.45	2.37	6.78	2.40	7.20
2.39	6.85	2.40	7.67	2.40	7.67
2.40	7.67				

15-series inlets

Cowling

x	b	c
0	2.43	2.43
.005	2.43	2.44
↕ 1.000		2.62
2.000		2.79
6.800	3.25	3.38
7.800	3.33	3.45
↕ 8.67	3.35	3.47

↕ Indicates straight-tapered section.

Spike

a	x		
	Inlet 1520	Inlet 1518	Inlet 1515
0[1]	-2.60	-2.28	-1.70
.80[1]	-.30	-.58	.00
.88	-.70	-.38	.20
.97	-.40	-.08	.50
1.11	.10	.42	1.00
1.36	1.10	1.42	2.00
1.59	2.10	2.42	3.00
1.79	3.10	3.42	4.00
1.98	9.10	4.42	5.00
2.16	5.10	5.42	6.00
2.22	5.46	5.78	6.36

Spacers

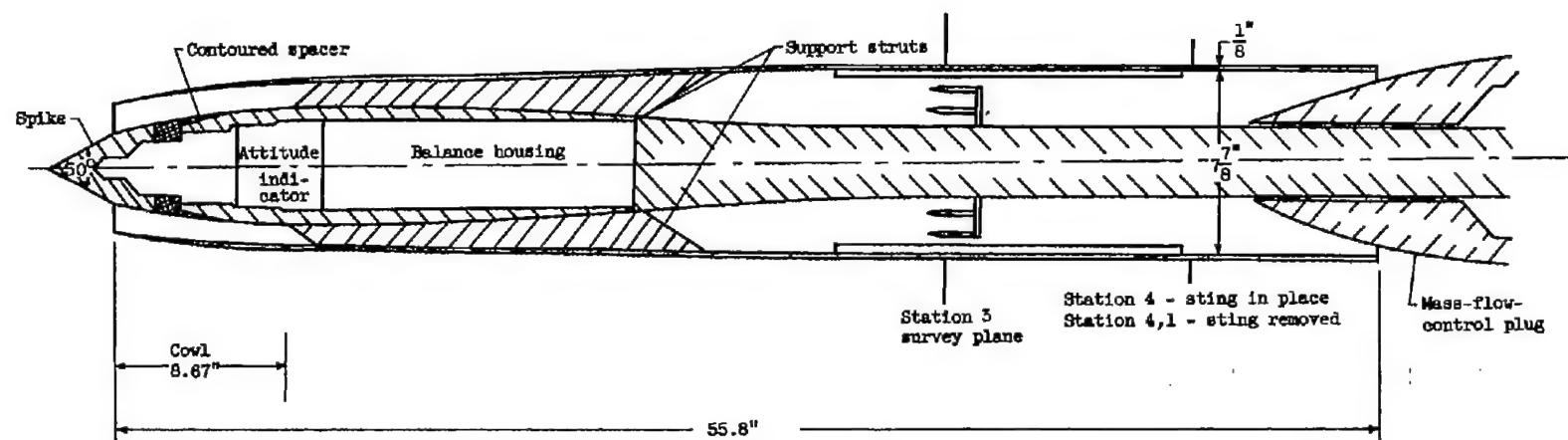| Inlet 1520			Inlet 1518			Inlet 1515	
x	a		x	a		x	a
	Contour	Cylinder		Contour	Cylinder		
5.46	2.22	2.22	5.78	2.22	2.22	----	----
6.36	2.35	2.22	6.36	2.32	2.22	6.36	2.22
6.50	2.36	2.24	6.50	2.33	2.24	6.50	2.24
7.00	2.39	2.33	7.00	2.38	2.33	7.00	2.33
7.50	2.40	2.39	7.50	2.40	2.39	7.50	2.39
7.67	2.40	2.40	7.67	2.40	2.40	7.67	2.40

[1] Region of 25° half-angle cone.
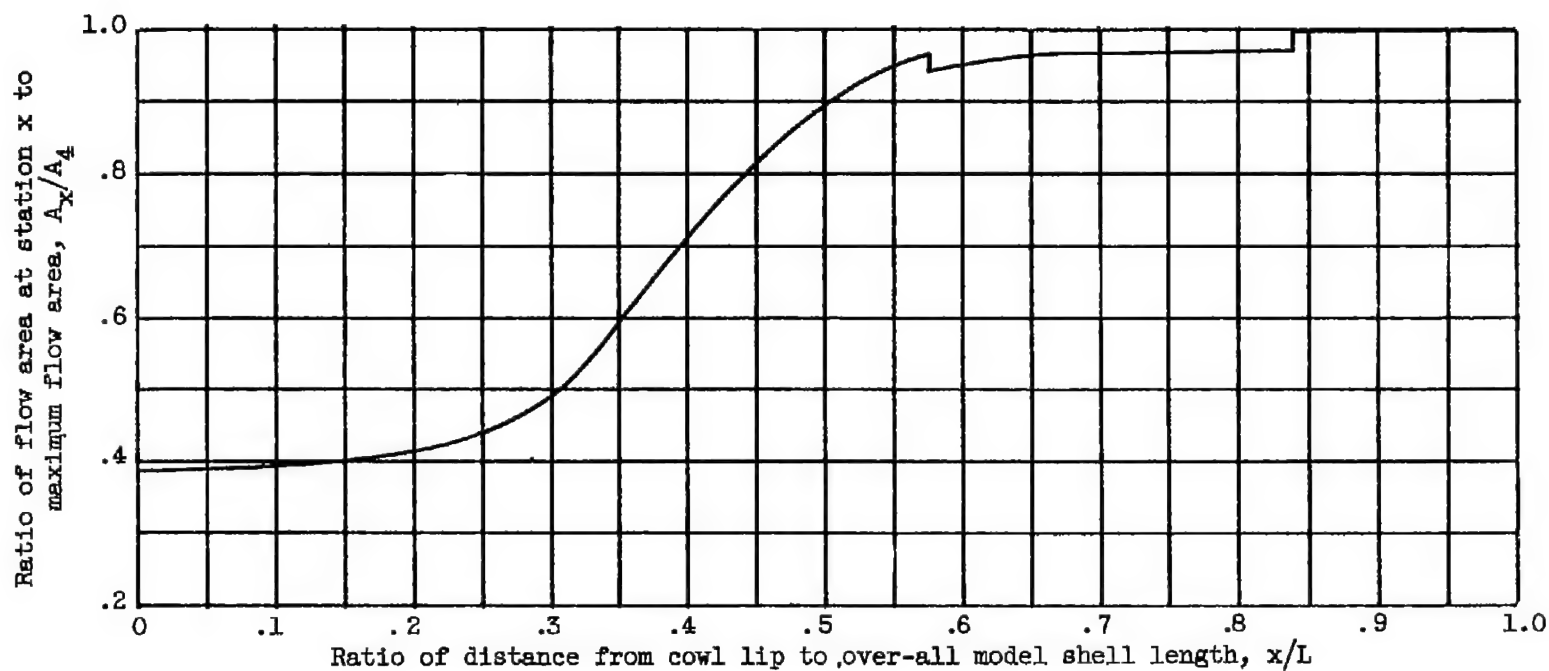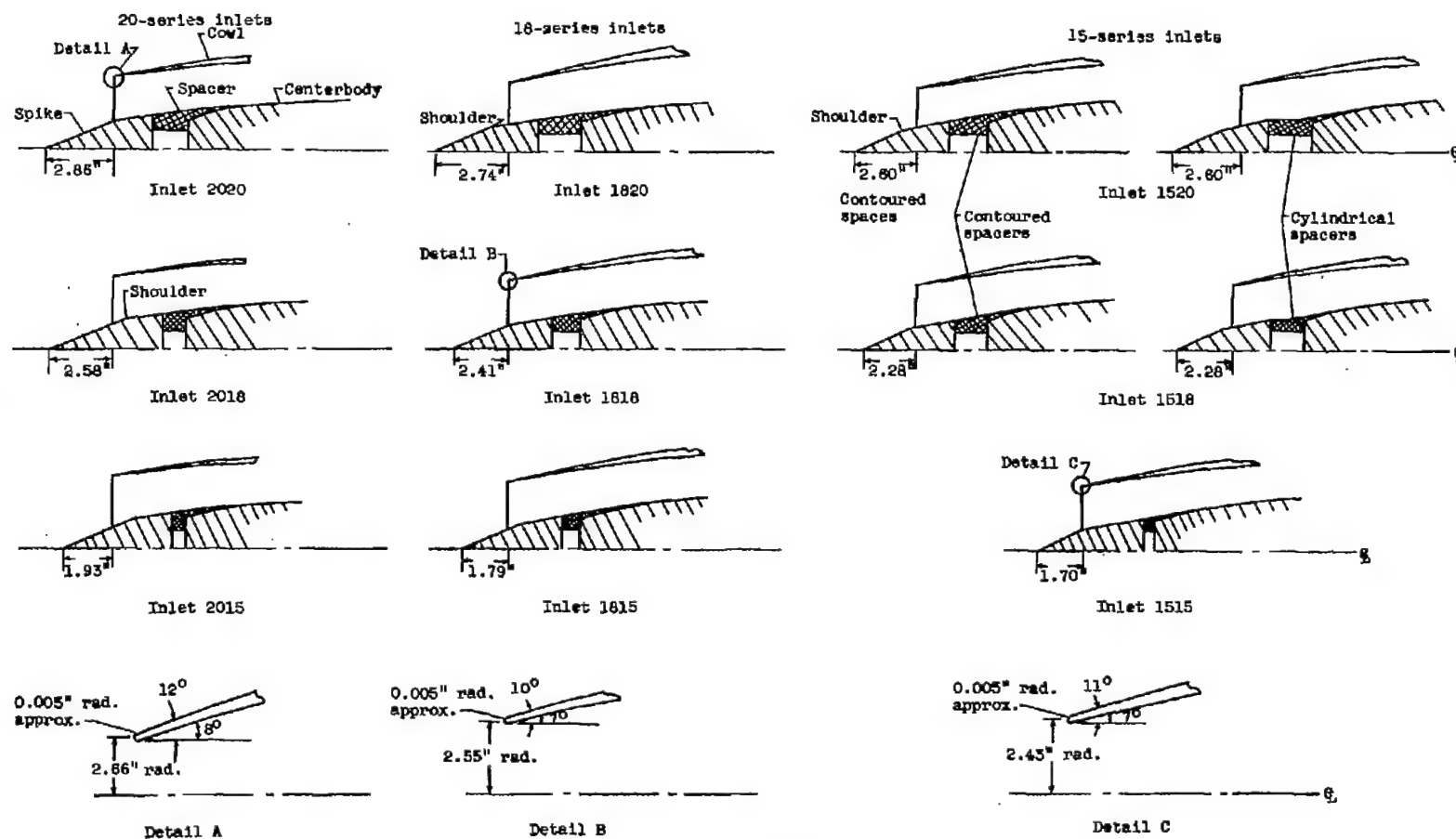
Figure 1. - Schematic drawing of diffuser model.

Figure 2. - Basic diffuser area variations for inlets 2020, 1818, and 1515.

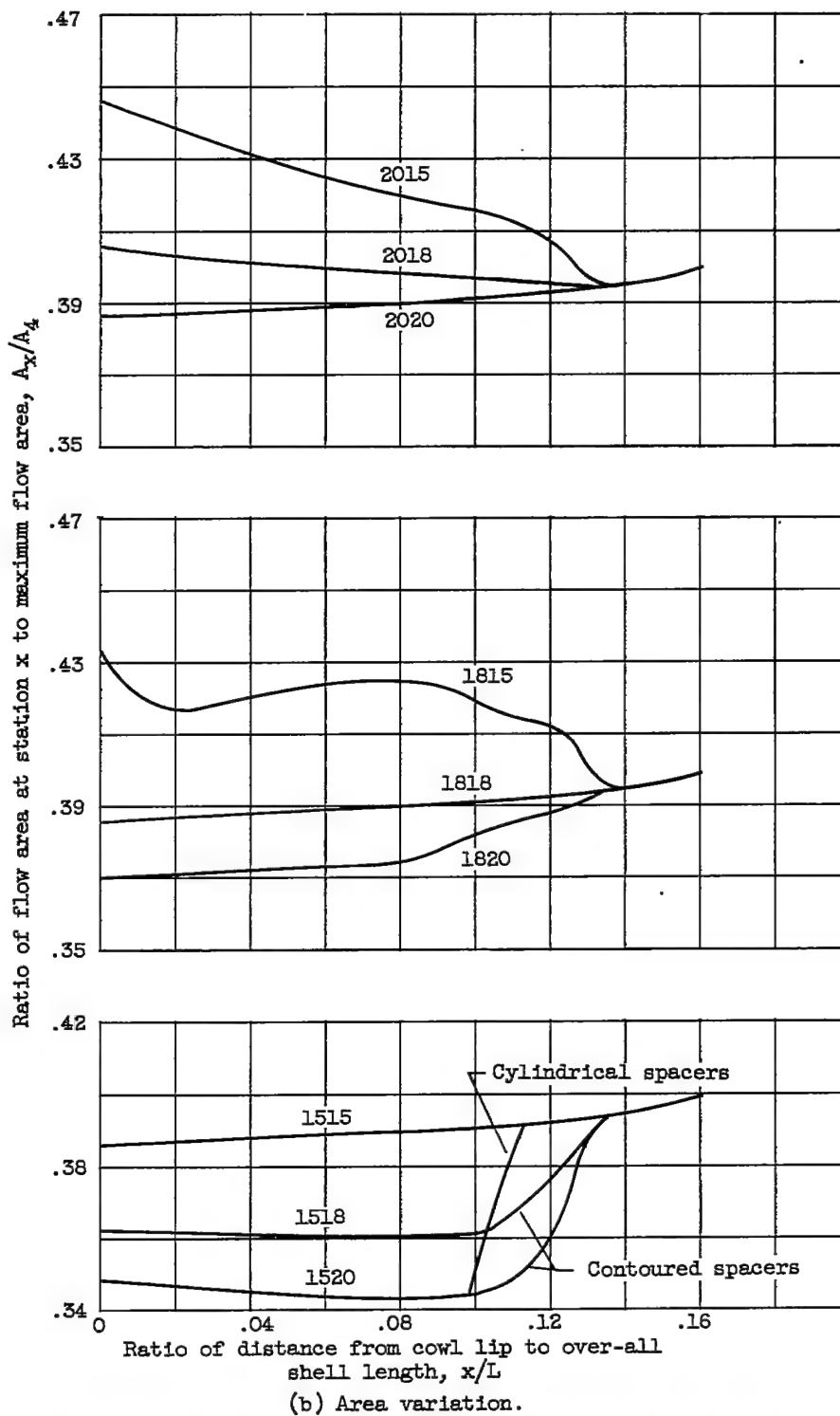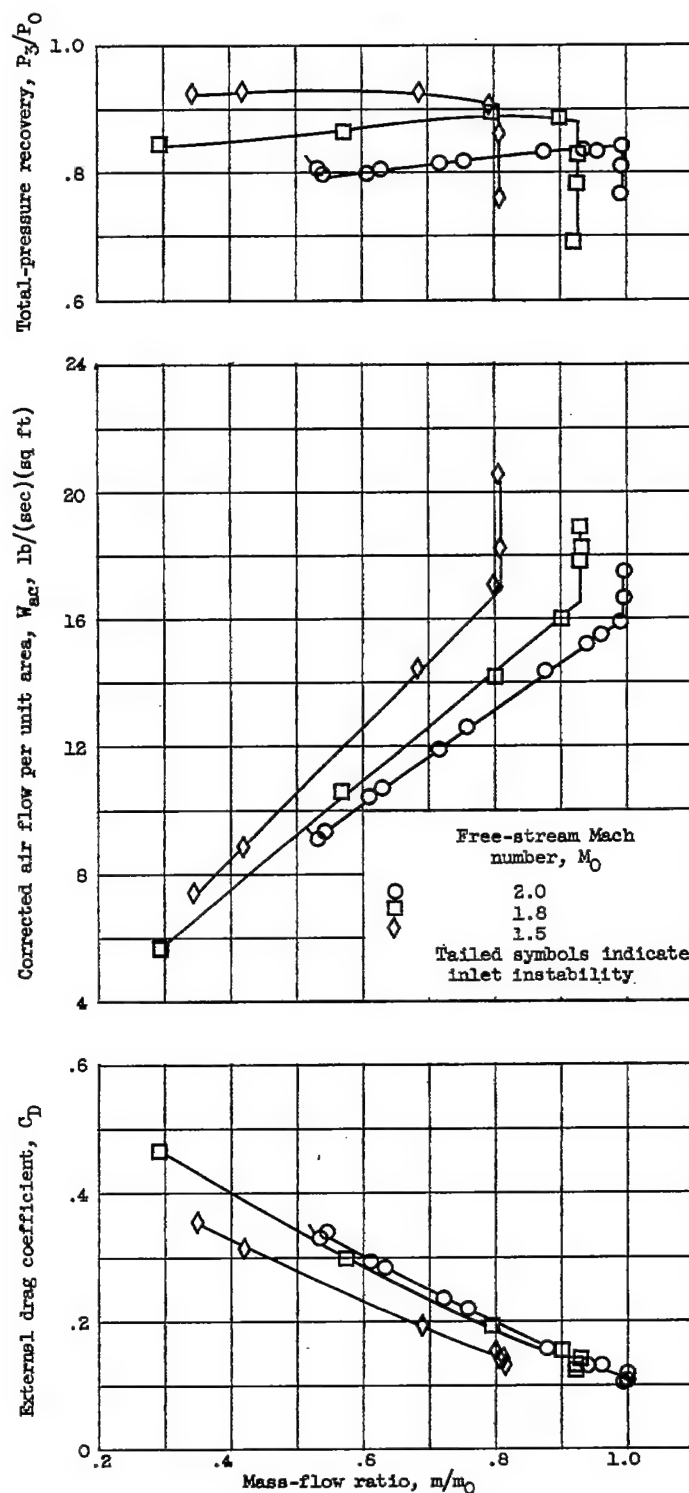(a) Schematic sketches.

Figure 3. – Contour and flow area details.

3206

(b) Area variation.
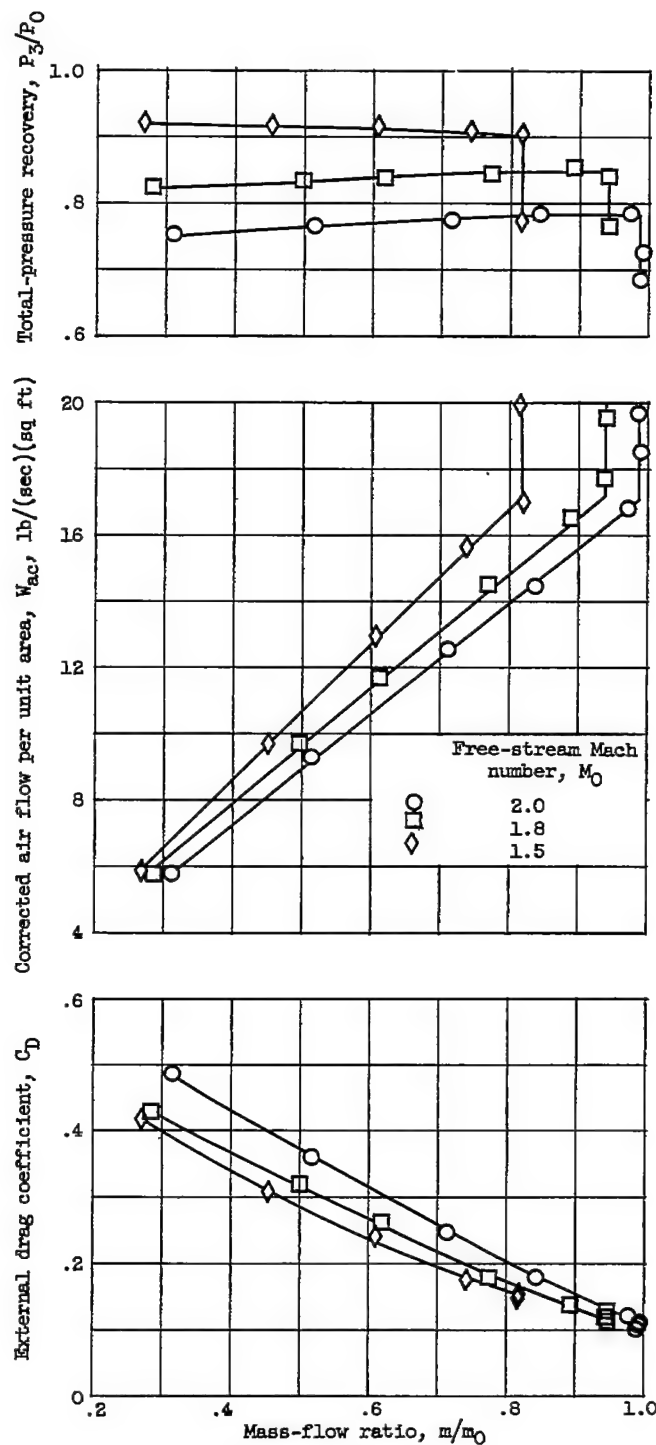
Figure 3. - Concluded. Contour and flow area details.

CONFIDENTIAL

3206

Free-stream Mach
number, M_0

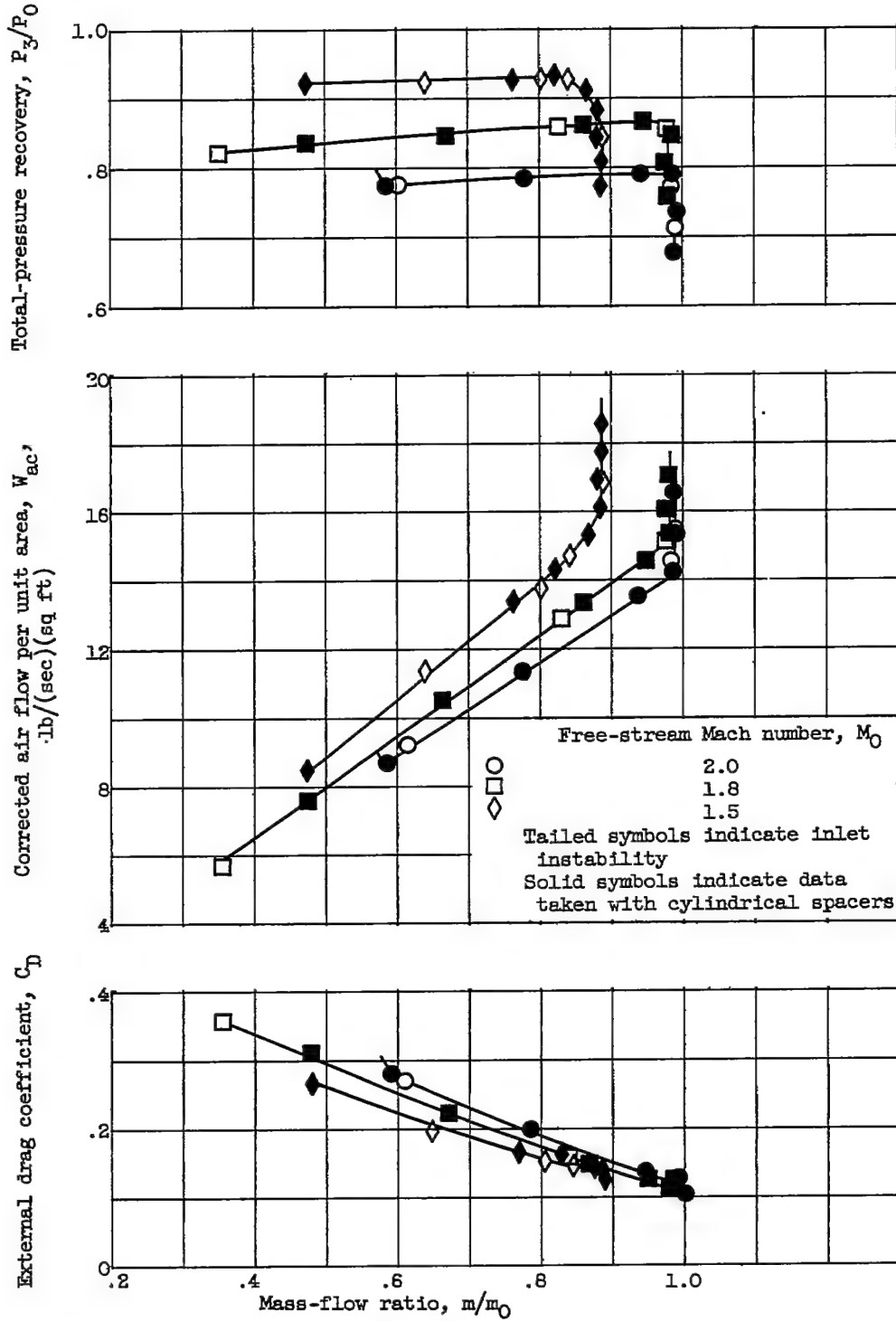|	
○	2.0
□	1.8
◇	1.5

Tailed symbols indicate
inlet instability

(a) Inlet 2020.

Figure 4. - Performance of 20-series inlets at
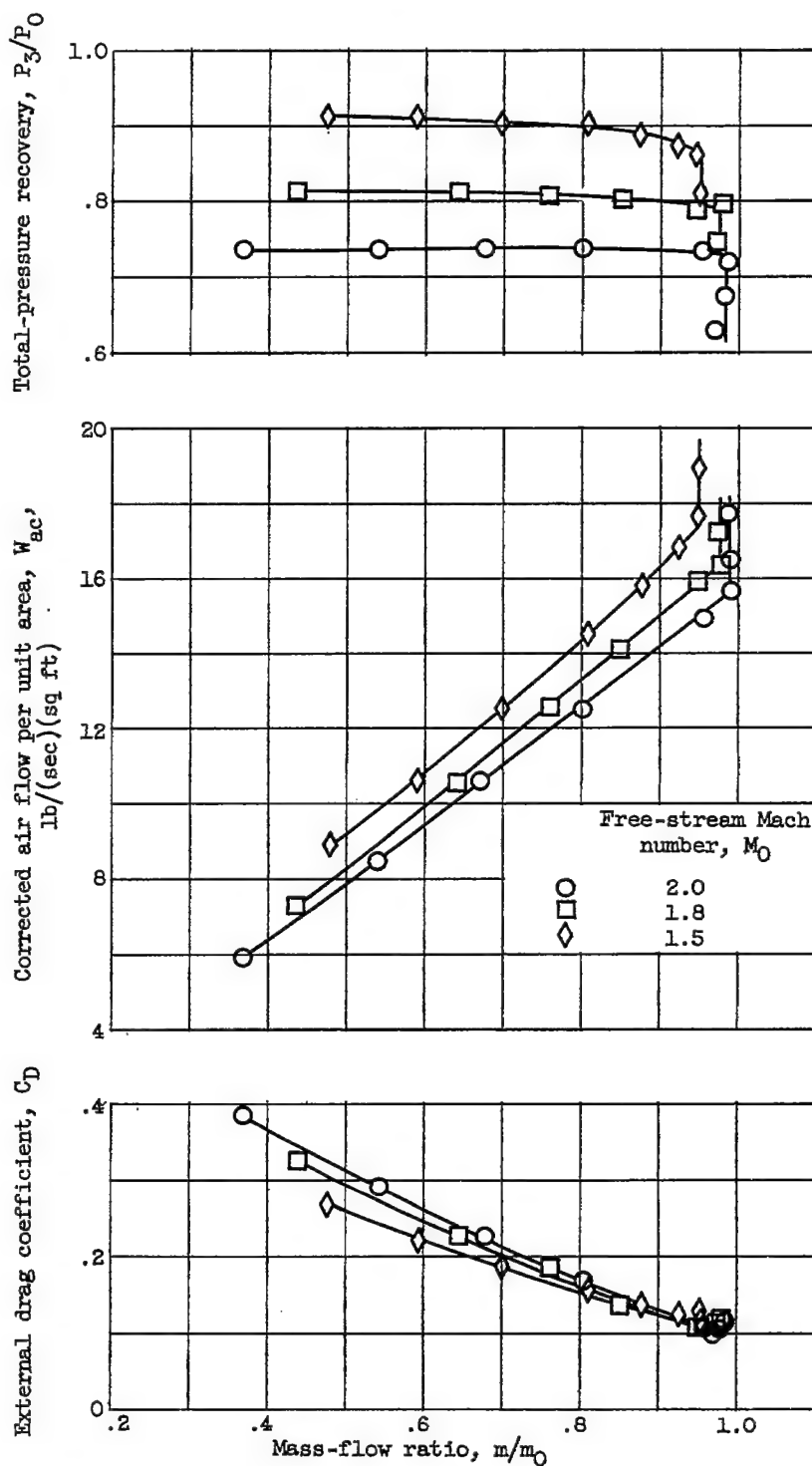zero angle of attack.

CONFIDENTIAL

3206

(b) Inlet 2018.

Figure 4. - Continued. Performance of 20-series inlets at zero angle of attack.
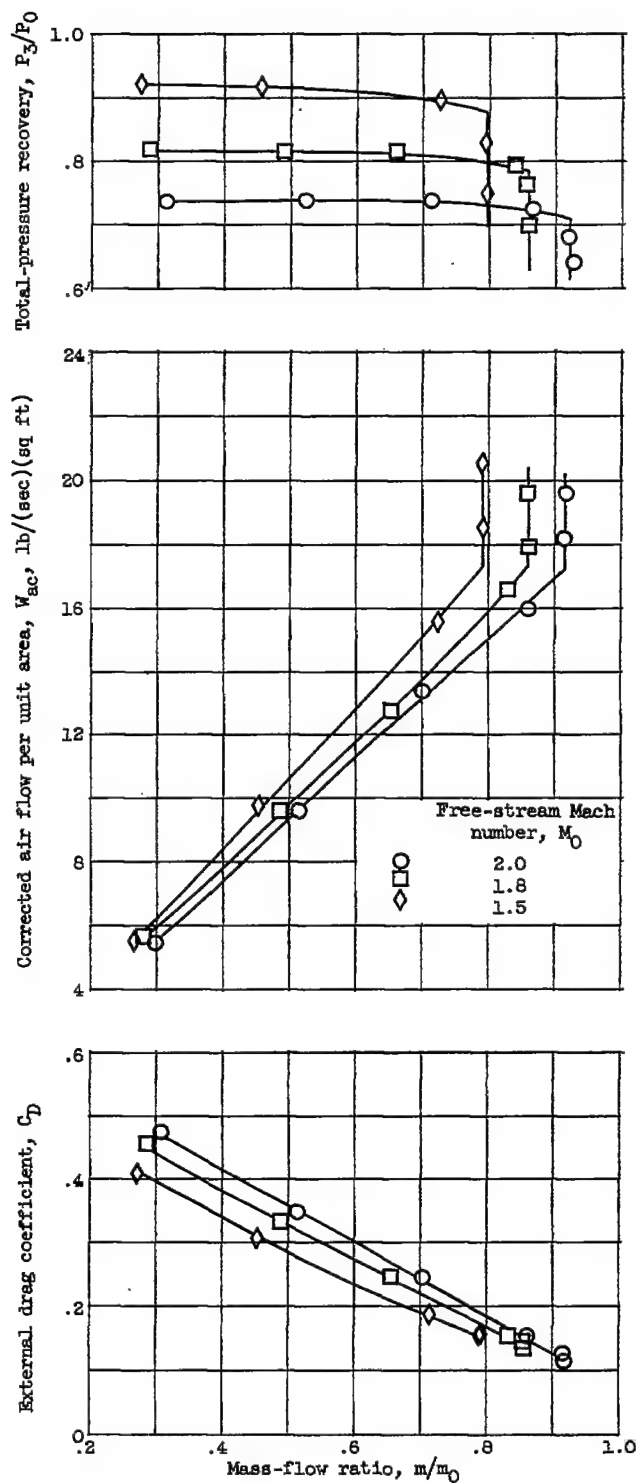
3206

(c) Inlet 2015.

Figure 4. - Concluded. Performance of 20-series
inlets at zero angle of attack.

3206

CK-3

Free-stream Mach number, M_0

○	2.0
□	1.8
◇	1.5

Tailed symbols indicate inlet instability

(a) Inlet 1820.
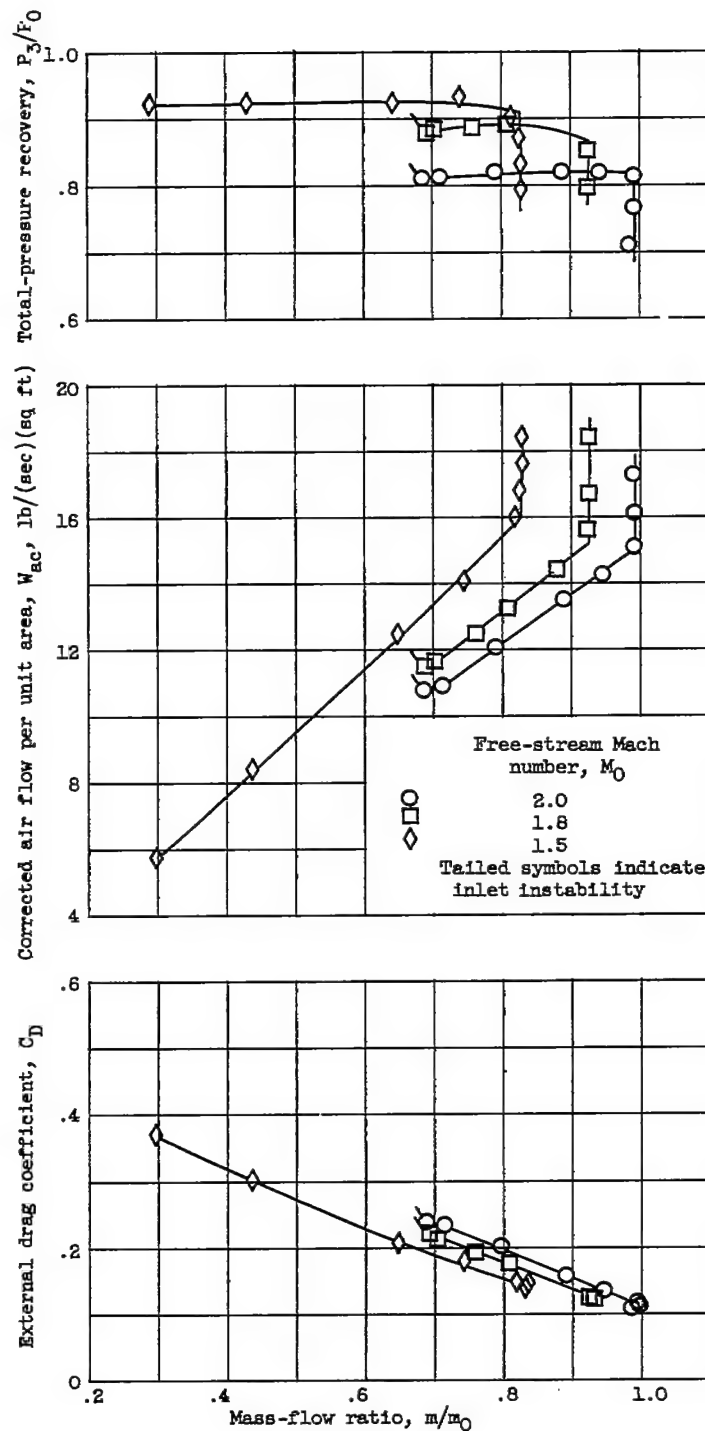
Figure 5. - Performance of 18-series inlets at zero angle of attack.
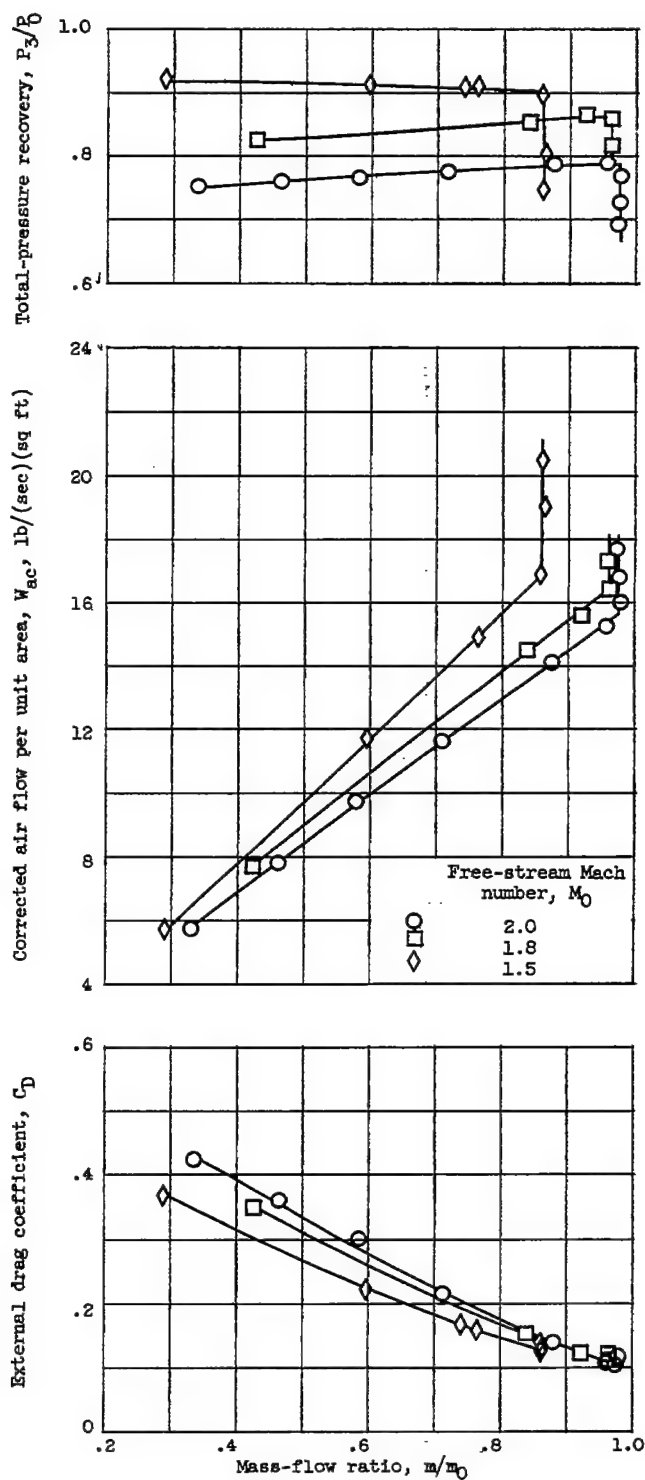
CONFIDENTIAL

(b) Inlet 1818.

Figure 5. - Continued. Performance of 18-series inlets at zero angle of attack.

CONFIDENTIAL

3206

CK-3 back

Free-stream Mach
number, M_0

○   2.0
□   1.8
◇   1.5

(c) Inlet 1815.
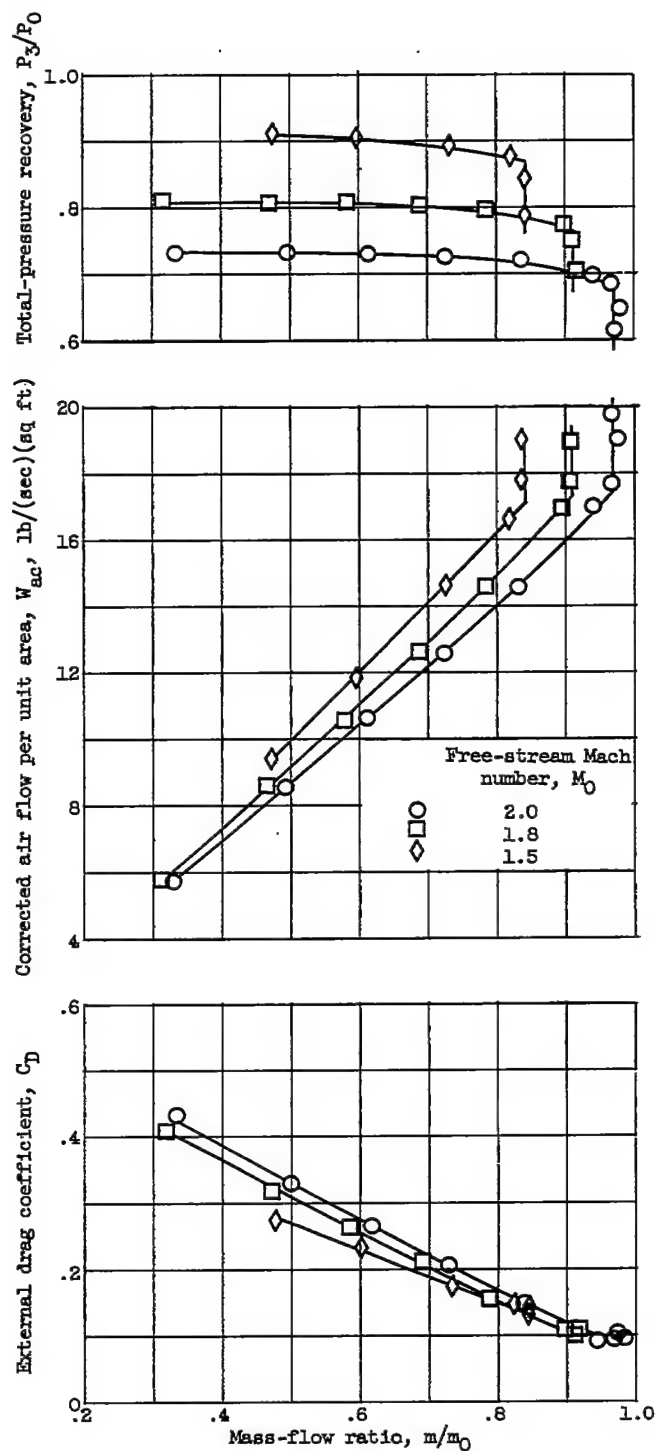
Figure 5. - Concluded. Performance of 18-series
inlets at zero angle of attack.

CONFIDENTIAL

Free-stream Mach number, M_0

○ □	2.0
	1.8
◇	1.5

Solid symbols indicate data
taken with cylindrical spacers
Tailed symbols and dashed curve
indicate inlet instability
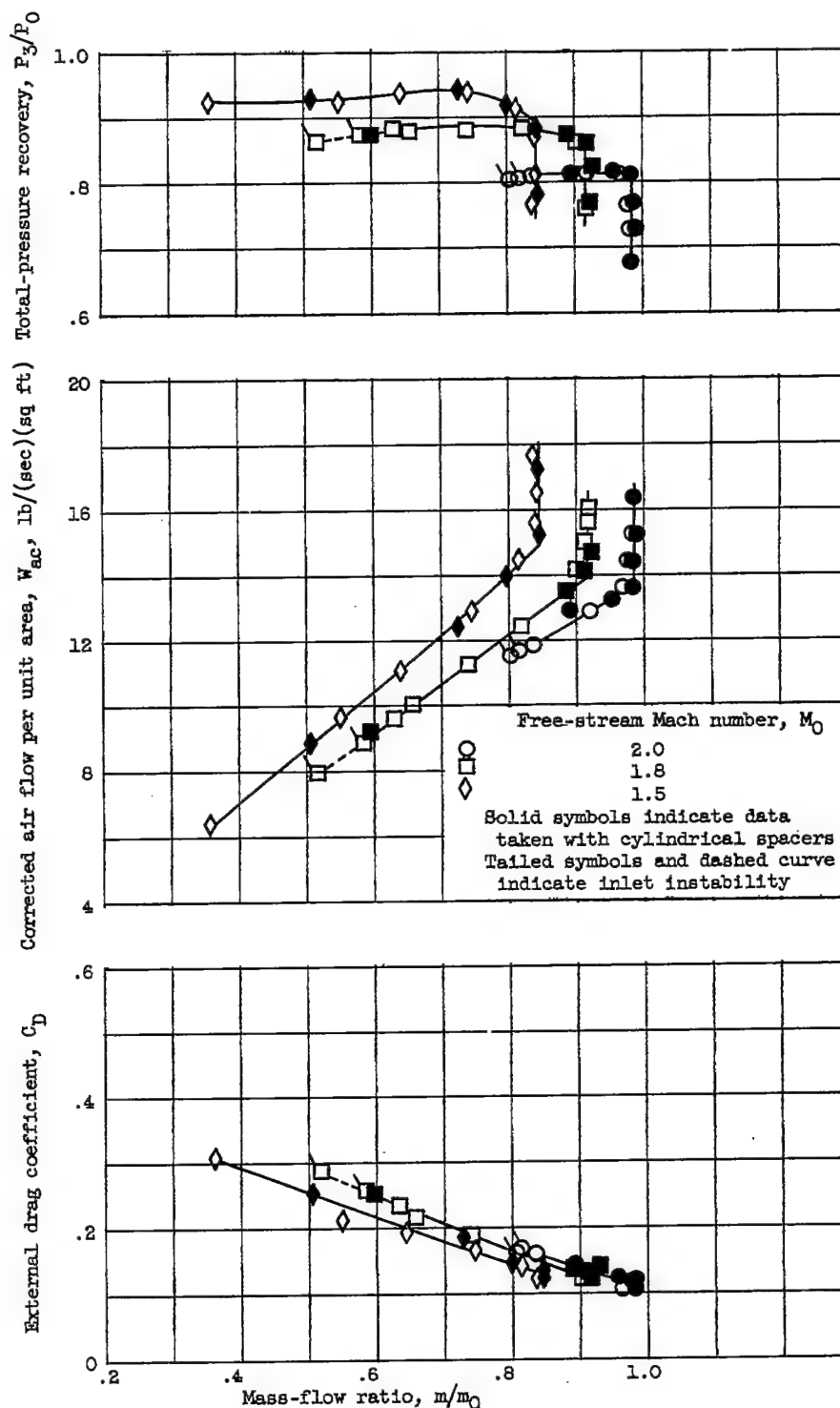
(a) Inlet 1520.

Figure 6. - Performance of 15-series inlets at
zero angle of attack.

CONFIDENTIAL

3206

Free-stream Mach number, M_0

○ 2.0
□ 1.8
◇ 1.5

Tailed symbols indicate inlet
instability
Solid symbols indicate data
taken with cylindrical spacers

(b) Inlet 1518.

Figure 6. - Continued. Performance of 15-series
inlets at zero angle of attack.

CONFIDENTIAL

3206

Figure 6. - Concluded. Performance of 15-series
inlets at zero angle of attack.

(c) Inlet 1515.

(a) Inlet 2020.   (b) Inlet 2018.   (c) Inlet 2015.
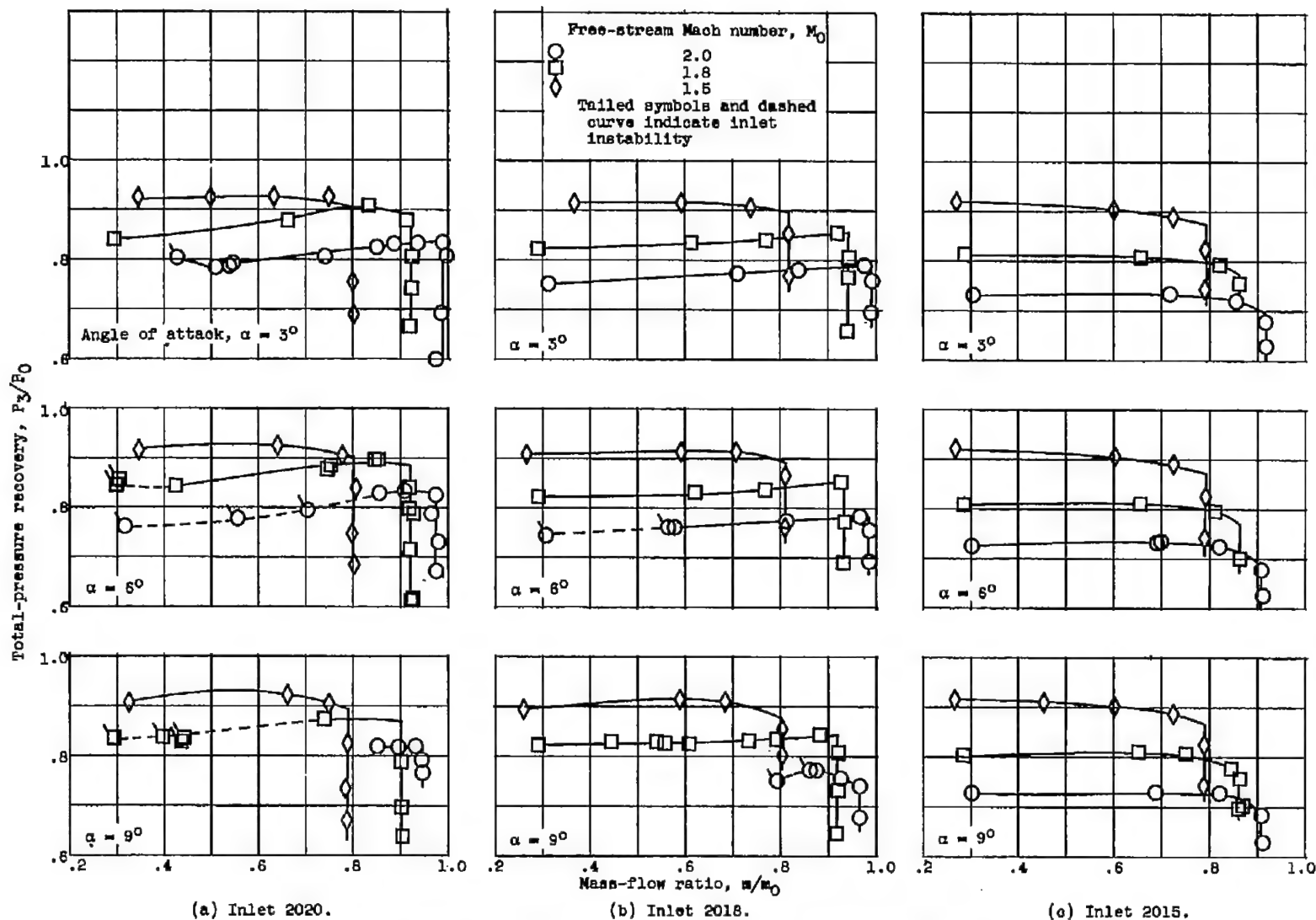
Figure 7. - Angle of attack performance of 20-series inlets.

(a) Inlet 1820.

(b) Inlet 1818.

(c) Inlet 1815.
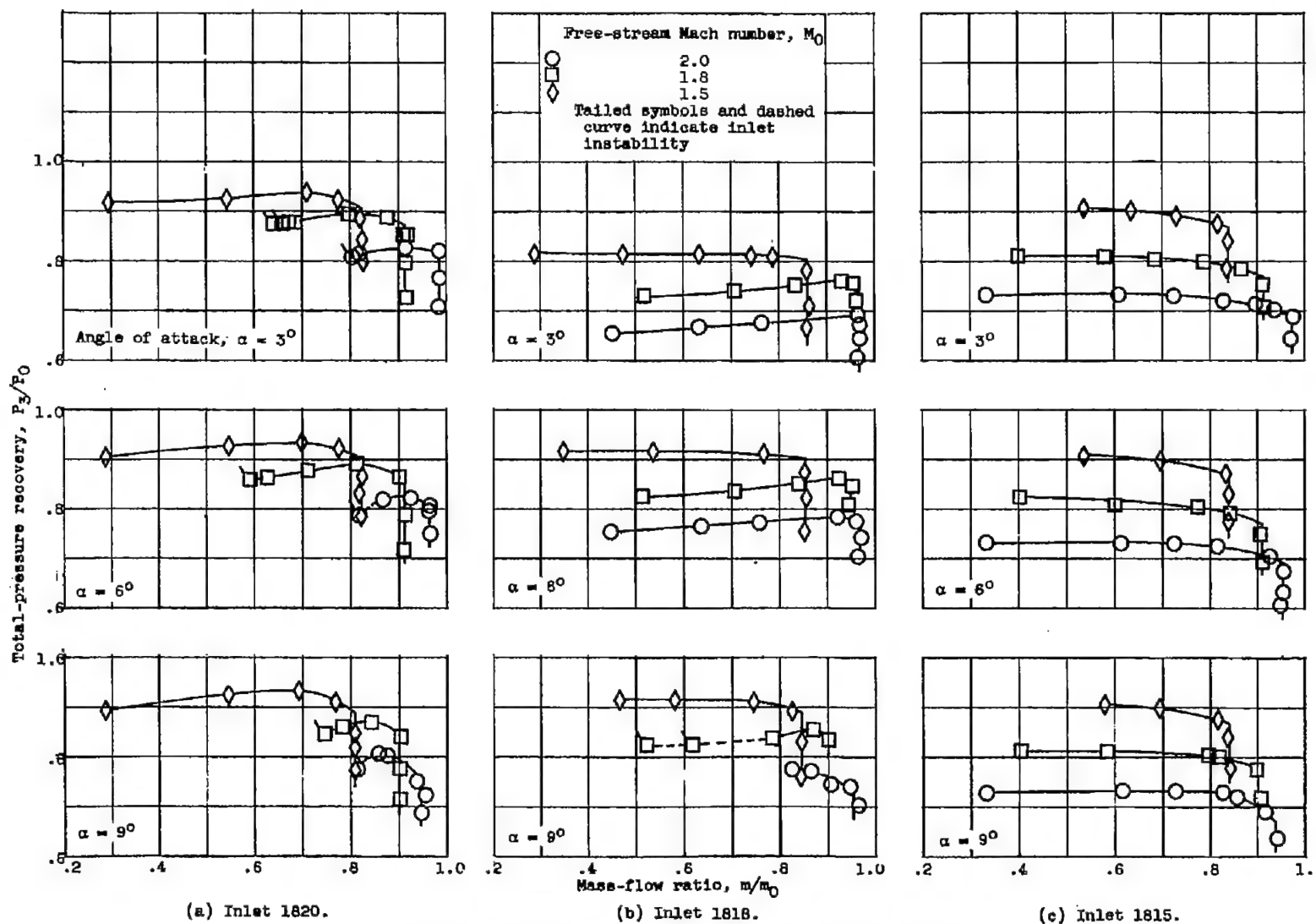
Figure 8. - Angle of attack performance of 18-series inlets.
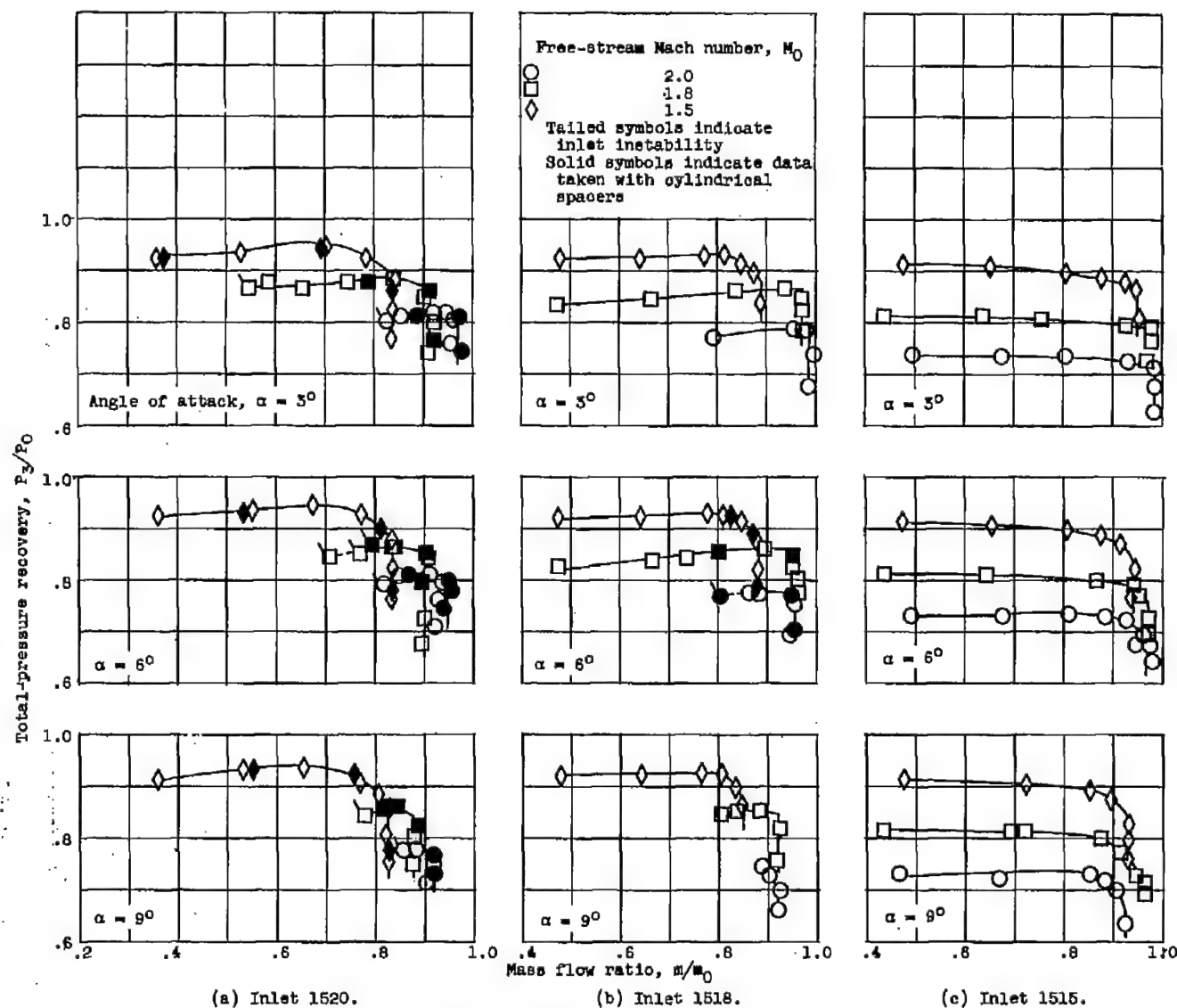
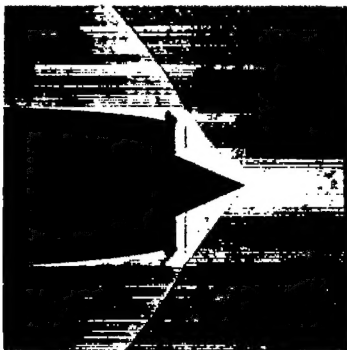Figure 9. - Angle of attack performance of 15-series inlets.
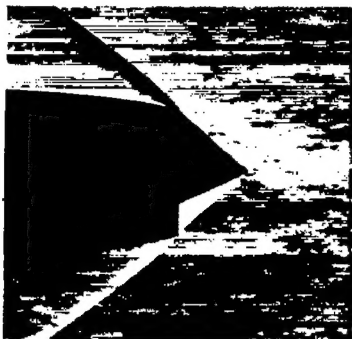
(a) Inlet 2020, without reexpansion.
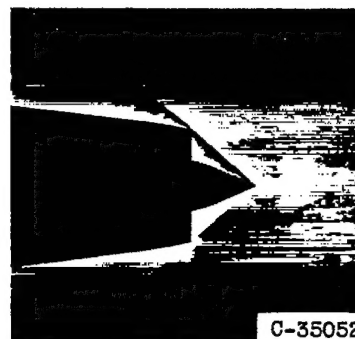
(b) Inlet 1520, with reexpansion.

Figure 10. - Effect of flow reexpansion over cone shoulder on inlet shock pattern for critical flow conditions at Mach 2.0.

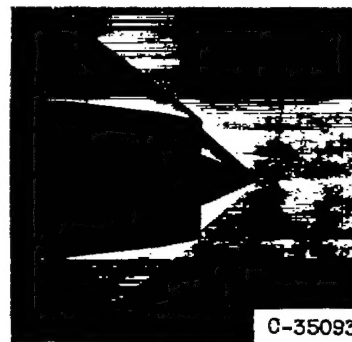(a) Inlet 2020, without internal contraction.

(b) Inlet 2018, with internal contraction.

Figure 11. - Effect of internal flow contraction on inlet shock pattern for critical conditions at Mach 1.5.

(a) Inlet 1820, oblique shock at cowl lip.

(b) Inlet 1818, oblique shock within cowl lip.

Figure 12. - Effect of oblique shock inside the cowl lip on inlet shock pattern for critical conditions at Mach 2.0.
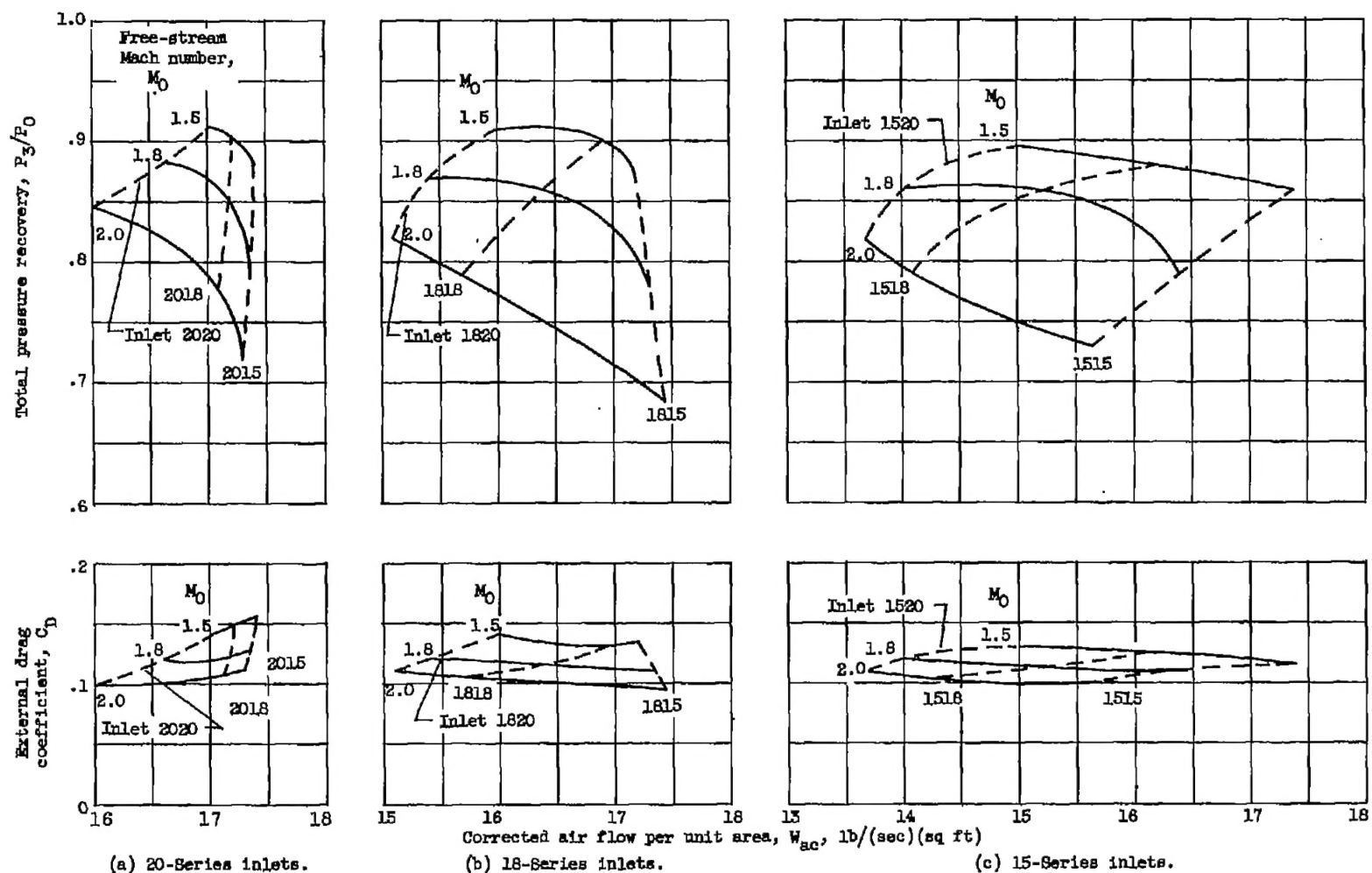
Figure 13. – Corrected air flow maps for critical operation at zero angle of attack.

(a) 20-Series inlets.
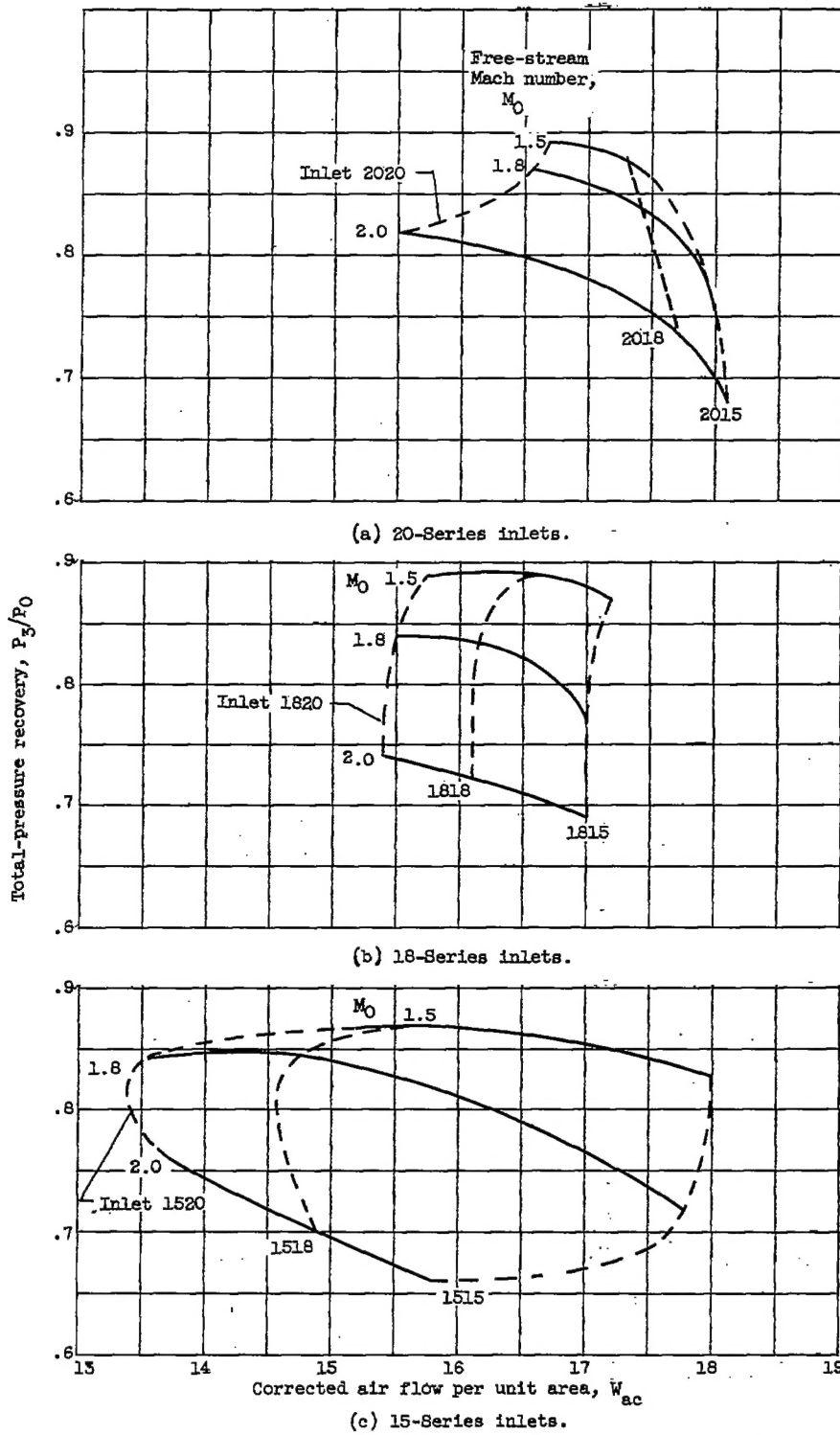
(b) 18-Series inlets.

(c) 15-Series inlets.

(a) 20-Series inlets.

(b) 18-Series inlets.

(c) 15-Series inlets.

Figure 14. - Corrected air flow maps for critical operation at 9° angle
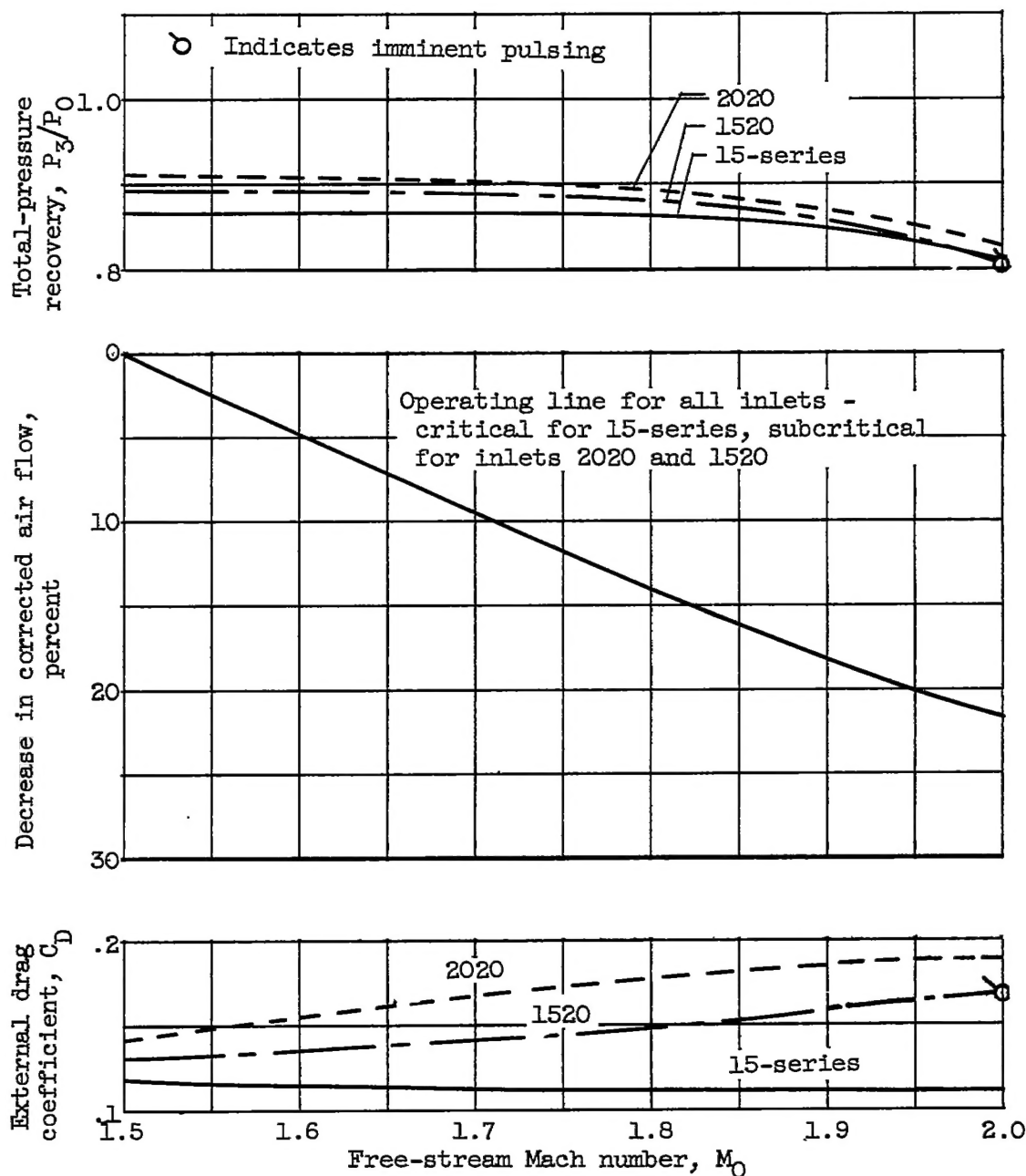of attack.

3206

Figure 15. - Performance comparison of fixed-geometry inlets with translating-cone inlet at zero angle of attack.